International Journal of Advanced Engineering and Technology Research
ISSN: 3106-8677 (Print), ISSN: 3106-8685 (Online) | Vol. 3, No. 3, 2026

Comparative Assessment of Carbon Nanotube and Steel Fiber Reinforcement in Recycled Aggregate Shotcrete

Yakun Kang

School of Civil Engineering, Henan Polytechnic University, Jiaozuo 454000, Henan, China

Abstract: Recycled coarse aggregate shotcrete (RCAS) offers a resource-efficient route for underground support, but adhered mortar, heterogeneous interfaces and brittle crack propagation limit its mechanical reliability. This study critically integrates two independent experimental investigations of multi-walled carbon nanotube (MWCNT) and steel-fiber (SF) modification to evaluate the complementary roles of matrix-scale densification and crack-scale bridging. The original experimental conditions are preserved while comparable strength, deformation, pore-structure and tensile-energy indicators are examined. In the MWCNT-modified mixtures, a dosage of 0.06 wt% yielded the highest reported 28 d compressive strength (38.25 MPa), whereas 0.09 wt% maximized the splitting-tensile (3.95 MPa) and flexural (4.88 MPa) strengths. Higher dosages reduced performance as dispersion deteriorated. In the separate SF-reinforced series, increasing recycled aggregate replacement from 0% to 100% reduced direct-tensile strength from 2.6 to 2.2 MPa, whereas increasing fiber content from 0% to 2% at 50% replacement increased tensile strength from 1.5 to 3.3 MPa. Together, these observations distinguish nano-scale hydration and pore refinement from fiber-mediated stress transfer after cracking. A mechanism-based reinforcement framework is proposed to balance constructability, strength, ductility and energy absorption. Because the two experimental programs differ in aggregate quality, mixture design and test conditions, combined MWCNT–SF effects remain a hypothesis requiring dedicated experimental validation.

Keywords: Recycled aggregate shotcrete, carbon nanotubes, steel fibers, interfacial transition zone, tensile behaviour, multi-scale reinforcement, mix design.

1. Introduction

Construction and demolition wastes provide a growing source of recycled concrete aggregate, while shotcrete remains essential for tunnels, underground caverns, mine roadways, slopes and rapid repairs. Their combination can reduce reliance on virgin aggregate, but the inherited mortar, pores and old interfacial transition zones (ITZs) of recycled aggregate complicate pumping, early-age strength and fracture resistance. The resulting weaknesses are not adequately characterized by compressive strength alone: crack initiation, deformation capacity and post-cracking load transfer are also important. Recent mesoscopic and fracture investigations show that the geometry of attached mortar and the mechanical quality of the ITZ influence local crack development and the macroscopic response [20, 21].

Li et al. [1] studied wet-mix recycled coarse aggregate shotcrete in which natural coarse aggregate was completely replaced by recycled coarse aggregate and MWCNTs were introduced as a nano-reinforcement. Their work linked rheology, spatial nanotube distribution, compressive strength, splitting-tensile strength, flexural strength, mercury-intrusion pore characteristics, SEM observations and XRD hydration products. The study is particularly useful because it treats shotcrete as a material-processing system rather than simply transferring conclusions from cast concrete. The authors showed that MWCNT effectiveness depends strongly on dosage and dispersion: beneficial nano-filling and crack-bridging dominate at low-to-moderate dosages, whereas agglomeration becomes detrimental when the dosage is too high.

Zhang et al. [2] examined a complementary reinforcement strategy: hooked steel fibers were added to recycled coarse aggregate shotcrete and direct-tension curves were measured across different strength grades, replacement ratios and fiber contents. Their reported peak stress, peak strain, modulus, tensile work and post-peak response establish an experimental basis for distinguishing crack initiation from crack bridging. Recent direct-tension and flexural tests on steel-fiber-reinforced recycled concrete likewise emphasize that tensile constitutive properties depend on the test configuration and fiber contribution [22].

These two investigations address different controlling mechanisms. MWCNTs, when sufficiently dispersed, primarily affect the hydration products, pore network and bond quality of the cementitious matrix and ITZs. Steel fibers, in contrast, become particularly important when a localized crack opens and bridging tractions must be sustained. Mesoscale studies confirm the sensitivity of recycled-concrete properties to old and new mortar phases [23]; more recent work combining carbon nanotubes with steel and PVA fibers in fully recycled aggregate concrete supports the physical rationale for multi-scale reinforcement while remaining distinct from a shotcrete-specific hybrid experiment [24].

The objective of the present study is therefore to establish a coherent, mechanism-based comparison of these reinforcement routes rather than merge the two experimental datasets into a single fictitious test matrix. Source-specific mixture variables and loading conditions are retained, reported properties are compared within their own experimental series, and nano- and macro-scale strengthening functions are related to practical shotcrete design objectives. The combined MWCNT–SF strategy proposed here is a design hypothesis; no new hybrid mixture or independent specimen test is claimed.

2. Research Basis and Experimental Methods

The analysis is grounded in two independent experimental investigations. Li et al. [1] used recycled coarse aggregate graded from 5 to 16 mm, a water–cement ratio of 0.50, and 440 kg/m³ of cement while varying MWCNT dosage from 0 to 0.15 wt%. Specimens prepared by wet spraying were tested at 1, 3, 7 and 28 d. Zhang et al. [2] investigated wet-sprayed SFRCAS at nominal strength grades C20–C40, recycled aggregate replacement ratios of 0%–100%, and steel-fiber volume fractions of 0%–2%, including direct-tension specimens with a 150 mm gauge length. Because the original specimens and loading protocols differed, cross-study comparison is restricted to compatible response indicators and mechanistic trends.

The source materials also reveal that recycled aggregate quality differed between the two programs. In Li et al. [1], the recycled aggregate had an apparent density of 2570 kg/m3, bulk density of 1341 kg/m3, water absorption of 2.58% and crushing index of 11.88%. In Zhang et al. [2], the corresponding recycled aggregate had an apparent density of 2520 kg/m3, bulk density of 1194 kg/m3, water absorption of 4.5% and crushing value of 14.3%. These differences are important because the response of RCAS cannot be interpreted solely by replacement ratio; recycled aggregate source quality changes the volume and weakness of old mortar, water demand, particle strength and ITZ characteristics. Related 4D CT observations of micro-steel-fiber-reinforced recycled concrete reveal how aggregate and fiber distributions influence internal cracking; their results are used here only as mechanistic context rather than combined with the two shotcrete datasets [25].

Table 1. Key recycled-aggregate characteristics and experimental variables in the two source experiments.

Property	Li et al. [1]	Zhang et al. [2]
Apparent density (kg/m^3)	2570	2520
Bulk density (kg/m^3)	1341	1194
Water absorption (%)	2.58	4.50
Crushing index/value (%)	11.88	14.30
Primary RCA variable	100% RCA + MWCNT dosage	RA replacement ratio + SF dosage

To compare different material properties without mixing incompatible strength scales, this study uses a dimensionless performance index based on a modified mixture and its corresponding control within the same experimental series. Values above unity indicate an increase relative to the control, whereas values below unity indicate a decrease. This normalization is used for comparison and visualization only; the source measurements retain their original units and are not treated as new tests.

The comparison deliberately avoids treating correlation as proof of a common causal law. For example, the MWCNT series used 100% recycled coarse aggregate, whereas the steel-fiber study changed the recycled aggregate replacement ratio. Their specimen geometries, curing conditions, loading configurations and admixture systems also differed. Therefore, the present analysis emphasizes directional trends and mechanisms that are internally consistent within each study, rather than claiming a single universal numerical optimum for all RCAS.

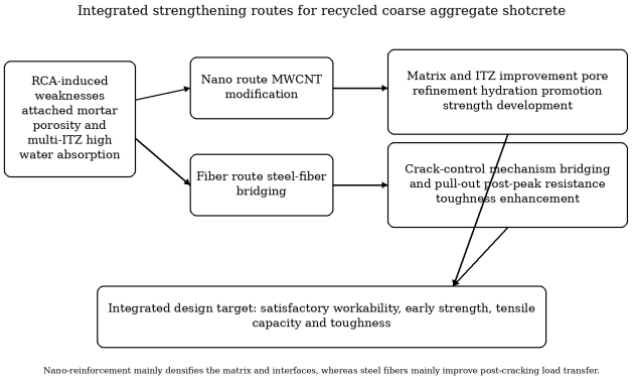


Figure 1. Integrated research framework used in this paper. The diagram summarizes the strengthening routes and target performance of RCAS based on Refs. [1] and [2].

3. Materials, preparation and test methods

3.1. Recycled Aggregate Characteristics and Implications

The two experimental programs used recycled coarse aggregates derived from crushed waste concrete, but the reported physical properties show that the aggregates were not equivalent. Li et al. [1] used a 5-16 mm recycled coarse aggregate with an apparent density of 2570 kg/m3, bulk density of 1341 kg/m3, water absorption of 2.58%, crushing index of 11.88% and an adhered-mortar content of 26.3%. Zhang et al. [2] reported an apparent density of 2520 kg/m3, bulk density of 1194 kg/m3, water absorption of 4.5% and crushing value of 14.3% for their recycled aggregate. In the latter study, the corresponding natural aggregate had an apparent density of 2700 kg/m3 and water absorption of only 0.8%. These differences quantitatively illustrate the characteristic features that distinguish recycled from natural coarse aggregate: lower packing density, more connected porosity and a larger capacity to remove free water from the fresh cementitious phase.

From a mechanics perspective, attached old mortar creates a multi-phase particle rather than a homogeneous stone inclusion. The recycled particle contains original natural aggregate, old mortar and an old aggregate-mortar ITZ; when it is incorporated into a new cementitious matrix, a second ITZ develops between the recycled particle and the new mortar. The resulting hierarchy of interfaces provides preferential locations for crack initiation, especially under tension. This structural interpretation is consistent with the tensile results reported by Zhang et al. [2], in which increasing the recycled-aggregate replacement ratio reduced peak tensile strength and modulus even while peak tensile strain increased. It is also consistent with the motivation for the MWCNT strategy of Li et al. [1], which aimed to densify pores and ITZ regions rather than merely increasing bulk matrix strength.

Water absorption has an equally important processing consequence. A recycled aggregate that is dry or partially dry can absorb mixing water rapidly, thereby reducing the effective water-binder ratio in the surrounding paste during mixing, pumping and spraying. If this moisture exchange is uncontrolled, two nominally identical mixtures can develop different rheology and hydration. Conversely, excessive pre-saturation can introduce surface water and locally weaken the new ITZ. The source studies handled this issue within their own preparation procedures, but the comparison shows why

moisture state should be recorded as a primary mixture parameter in future RCAS research rather than treated as a minor material detail.

Table 2. Recycled-aggregate characteristics reported in the two source studies.

Parameter	Li et al. [1] RCA	Zhang et al. [2] RA	Interpretation
Apparent density	2570 kg/m^3	2520 kg/m^3	Both lower than typical natural aggregate
Bulk density	1341 kg/m^3	1194 kg/m^3	Indicates looser packing / attached mortar
Water absorption	2.58%	4.5%	Higher absorption increases fresh-state sensitivity
Crushing index/value	11.88%	14.3%	Second aggregate was mechanically weaker
Particle size	5-16 mm	<=15 mm	Both compatible with wet-shotcrete grading

3.2. MWCNT Mixture Design and Spraying Procedure

Li et al. [1] adopted 100% replacement of natural coarse aggregate with recycled coarse aggregate so that the influence of MWCNT dosage could be isolated against a fully recycled control. Five modified groups were prepared with MWCNT dosages of 0.03, 0.06, 0.09, 0.12 and 0.15 wt%, together with an ordinary recycled coarse aggregate shotcrete control. The water-cement ratio was fixed at 0.50 and the cement dosage at 440 kg/m3. Particle-size distribution was designed using Fuller grading, and the mixture proportions were checked against the requirements of the Chinese technical code for ground anchorage and shotcrete support. This experimental design is especially valuable for identifying a dosage window because the main compositional variable is the nanomaterial content rather than a simultaneous change in aggregate replacement.

The dispersion route was a combined process of surface non-covalent modification, mechanical stirring and ultrasonic treatment. Polyvinylpyrrolidone was used as a surfactant, followed by approximately 20 min of physical stirring and 30 min of ultrasonic treatment. The underlying reason is that MWCNTs possess a very high specific surface area and strong van der Waals attraction; without sufficient dispersion energy, increasing the nominal dosage can increase the size and frequency of nanotube clusters instead of increasing the amount of mechanically active nanotube surface. The later CT and SEM results in the source paper confirm that this processing issue was not theoretical: distribution became distinctly more scattered at 0.12 and 0.15 wt%.

Wet-mix spraying was carried out using a three-cylinder pulseless concrete sprayer connected to an approximately 80 m delivery line. A variable-addition device controlled the MWCNT suspension supply according to pipeline pressure. The sprayed wall was 0.6 m by 0.6 m by 0.12 m, and after 24 h the material was demolded and cut into 100 mm cubes for compressive and splitting-tensile tests and 100 mm by 100 mm by 400 mm prisms for flexural testing. Specimens were tested at 1, 3, 7 and 28 d. This preparation route is important because the modified material experienced pumping, acceleration and impact compaction rather than simple casting; therefore, the resulting dispersion and pore structure are representative of a genuine shotcrete process within the limitations of the laboratory setup.

3.3. Steel-fiber Mixture Variables and Tensile Specimens

Zhang et al. [2] used a factorial-style program that separated three variables: concrete strength grade, recycled aggregate replacement ratio and steel-fiber volume fraction. The strength-grade series included C20, C30 and C40 at 50% recycled aggregate and 1% steel fiber. The recycled-aggregate series used 0%, 30%, 50%, 70% and 100% replacement at C30 and 1% fiber. The fiber series used 0%, 0.5%, 1%, 1.5% and 2% at C30 and 50% recycled aggregate. This design provides a useful basis for identifying whether a change in tensile response is caused primarily by the matrix, the recycled aggregate fraction or the bridging reinforcement.

The steel fibers were hooked-end fibers with an average length of 35 mm, equivalent diameter of 0.75 mm, aspect ratio of 46.7 and tensile strength of 1128 MPa. The fibers were therefore long enough to bridge a localized crack and mechanically anchored by their end geometry. Unlike MWCNTs, which act within paste-scale pores and microcracks, these fibers interact with cracks at the millimeter scale. This difference in characteristic length scale is one of the central reasons the two strengthening approaches are complementary rather than interchangeable.

The SFRCAS was produced by wet spraying into large panels measuring 1200 mm by 550 mm by 150 mm. The nozzle was maintained approximately perpendicular to the target surface and about 1 m away, and the panels were subsequently cured and sawn into the required specimens. The direct-tension specimens had a 150 mm by 150 mm cross section, an overall length of 550 mm and embedded HRB400 steel bars at both ends. A 150 mm gauge length was selected so that tensile cracking would occur in the measured region while avoiding excessive end effects. The use of large sprayed panels before cutting is particularly relevant because it preserves key features of sprayed placement, including particle impact, compaction, fiber orientation and possible rebound-induced changes in local composition.

3.4. Mechanical and Microstructural Measurements

Recent interface-bond experiments on nanoparticle-modified fiber–cement systems further underline the importance of matrix composition and fiber spacing [26].

The MWCNT study combined conventional strength testing with several microstructural methods. Compressive and splitting-tensile strengths were measured on 100 mm cubes, while flexural strength was obtained from 100 mm by 100 mm by 400 mm prisms. X-ray computed tomography was used on small cored specimens to locate nanotube-rich features and reconstruct their three-dimensional spatial distribution. Mercury intrusion porosimetry quantified total pore volume, average pore diameter, most probable pore size and porosity. SEM observations were used to identify nanotube morphology, crack bridging, pull-out and agglomeration, and XRD was used to compare hydration-product signatures at 28 d. The benefit of this multi-method approach is that macroscopic strength changes can be checked against independent evidence from pore structure and

hydration.

The steel-fiber study focused on the complete uniaxial tensile response. A servo-hydraulic universal testing machine was used with force control in the early ascending stage and displacement control as the peak approached. Longitudinal deformation was recorded using LVDT sensors. Tensile strength was calculated from the maximum tensile load divided by the effective cross-sectional area. Tensile modulus was derived from the stress-strain response at one-third of failure stress, while tensile work was obtained from the area under the load-deformation curve up to a prescribed displacement limit. In this way the study distinguished peak resistance, stiffness, deformation capacity and energy absorption instead of reducing performance to a single tensile-strength value.

Taken together, the two test programs cover complementary parts of the material response. The MWCNT program provides a strong link between fresh rheology, microscopic structure and static strengths over age. The SFRCAS program provides direct evidence of crack evolution and post-peak load transfer. Their combination therefore permits a more complete conceptual description of RCAS behavior than either study alone, but it remains essential to keep the original boundary conditions separate when quantitative values are compared.

3.5. Data Normalization and Performance Indicators

The two experiments employed different control mixtures, specimen sizes and performance metrics. Accordingly, comparisons are based on within-series normalization rather than direct pooling of absolute strengths. The normalized performance index is defined below; it does not make distinct loading modes or test methods physically equivalent.

$$I_X = \frac{X_i}{X_{\text{ref}}} \tag{1}$$

Where I_x is the normalized performance index for property X; X_i is the value for the modified mixture; and Xref is the control value within the same experimental series. The index is dimensionless.

For MWCNT-modified RCAS, the most useful references are the unmodified ORCAS strengths and pore parameters. For the recycled-aggregate replacement series of SFRCAS, the 0% replacement mixture provides a natural reference for strength, strain and modulus, while the toughness quantities are compared in their original units because they exhibit a non-monotonic optimum. For the steel-fiber series, the fiber-free mixture is a clear reference for tensile strength, strain and modulus, but tensile work cannot be normalized to the fiber-free specimen because the brittle failure did not produce a comparable post-peak energy value. These restrictions are explicitly maintained in the reconstructed figures.

4. MWCNT Modification: Fresh-State Behavior and Mechanical Properties

4.1. Fresh-state Behavior and Processing Constraints

Fresh-state behavior is a first-order constraint for any shotcrete modification because a mixture that cannot be pumped, transported and atomized consistently cannot deliver its intended hardened-state performance. Li et al. [1] reported that increasing MWCNT dosage reduced slump while increasing relative yield stress and relative plastic viscosity. The mechanism was attributed to the extremely large specific surface area and adsorption capacity of MWCNTs, which bind free water, increase particle interaction and promote agglomeration when concentration rises. The recycled aggregate itself also absorbs water rapidly; consequently, nano-addition and recycled-aggregate water demand act in the same direction with respect to free-water reduction.

At low dosage, the surfactant used to disperse MWCNTs partly offsets this negative rheological effect. Li et al. [1] used a combined process involving non-covalent surface modification, mechanical stirring and ultrasonic treatment. They noted that the fresh properties of the low-dosage mixtures remained workable because the surfactant improved cement-particle dispersion. This is an important processing lesson: the optimal MWCNT dosage is not an intrinsic material constant but depends on the dispersion system, mixing energy, nanotube morphology, water-reducer system, aggregate absorption state and pumping history.

The fiber-reinforced study [2] highlights a parallel issue at a larger scale. Steel fibers increase internal obstruction and can lower workability, particularly when the recycled aggregate has high absorption and irregular morphology. Zhang et al. controlled the work state using slump and strength indicators and adopted a wet-sprayed large-panel procedure with the nozzle approximately 1 m from the surface. The source paper emphasizes that field-realistic spraying is essential because rebound and orientation can alter the spatial distribution of both aggregate and reinforcement.

The practical consequence is that mechanical enhancement cannot be optimized independently of construction rheology. MWCNTs require a dispersion window in which enough nanotubes are present to create a connected reinforcement network but not enough to form persistent agglomerates. Steel fibers require a dosage and geometry that provide crack bridging without producing fiber balls, excessive pumping resistance or unstable rebound. For recycled aggregate, preconditioning of moisture and a consistent absorption protocol are equally important because otherwise the effective water-binder ratio can change during mixing and pumping. These processing variables should be treated as controlled design parameters rather than secondary laboratory details.

4.2. Effect of MWCNT Dosage on Mechanical Properties

4.2.1. Compressive Strength Response

The compressive-strength dataset in Li et al. [1] displays a clear rise-and-fall response with MWCNT dosage. At 28 d, the control ORCAS reached 32.11 MPa. Strength increased to 34.95 MPa at 0.03 wt% and reached 38.25 MPa at 0.06 wt%, before decreasing to 36.71 MPa at 0.09 wt%, 34.55 MPa at 0.12 wt% and 28.61 MPa at 0.15 wt%. The authors reported a maximum 28 d compressive-strength increase of 20.39%. The same non-monotonic pattern appeared at earlier ages, and the greatest compressive response occurred at 0.06 wt% across 1, 3, 7 and 28 d.

This trend is consistent with competing beneficial and detrimental processes. At low-to-moderate dosage, dispersed nanotubes can fill microvoids, provide nucleation surfaces for hydration products, bridge very small cracks and improve stress transfer across the cementitious matrix. Once the dosage exceeds the capacity of the dispersion system, van der Waals attraction promotes agglomerates. Such agglomerates

behave less like distributed reinforcement and more like heterogeneous inclusions, creating local defects and preventing uniform hydration. The 0.15 wt% mixture therefore fell below the control at all reported ages, demonstrating that 'more nanomaterial' is not equivalent to 'more reinforcement.'

4.2.2. Splitting-tensile and Flexural Strength

Investigations of recycled-fiber shotcrete under cryogenic temperatures highlight the sensitivity of mechanical response to operating environment, but those results cannot be used to infer ambient-temperature behavior for the present mixtures [27].

The optimum dosage shifts slightly when tensile-dominated properties are considered. The 28 d splitting-tensile strength increased from 3.05 MPa for ORCAS to 3.95 MPa at 0.09 wt% MWCNT, for which Li et al. [1] reported a 29.43% increase. The 28 d flexural strength similarly increased from 4.05 MPa to 4.88 MPa at 0.09 wt%, corresponding to a reported increase of 20.52%. In contrast, 0.15 wt% produced 2.75 MPa splitting-tensile strength and 3.64 MPa flexural strength, both below the unmodified control.

The fact that compressive strength peaked at 0.06 wt% while splitting and flexural strengths peaked at 0.09 wt% is mechanistically informative. Compressive strength is strongly governed by matrix compactness and defect population; once the pore-refinement and hydration benefits are maximized, additional nanotubes can quickly become detrimental. Tensile and flexural resistance, however, also benefit from pull-out, bridging and frictional energy consumption along developing microcracks. A modestly higher nanotube population can therefore continue to improve crack resistance even after the compressive optimum has been passed, provided dispersion has not deteriorated severely.

Table 3. Selected 28 d strength results reported by Li et al. [1].

28 d property	ORCAS	Best MWCNT mixture	Reported change
Compressive strength	32.11 MPa	38.25 MPa at 0.06 wt%	+20.39%
Splitting tensile strength	3.05 MPa	3.95 MPa at 0.09 wt%	+29.43%
Flexural strength	4.05 MPa	4.88 MPa at 0.09 wt%	+20.52%

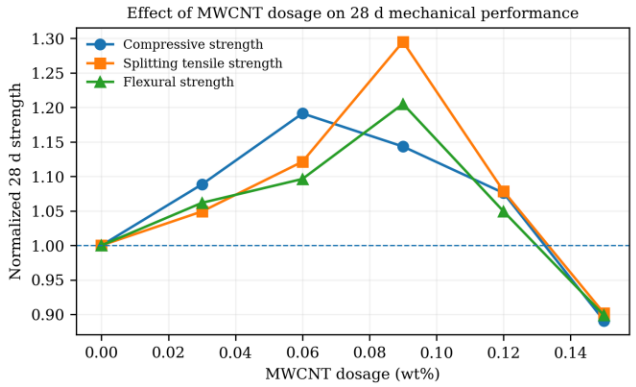


Figure 2. Normalized 28 d strength response reconstructed from the numerical data reported by Li et al. [1].

4.3. Age-dependent Strengthening Performance

The source data indicate that the relative benefit of MWCNTs is generally more pronounced at early age. For the 0.06 wt% mixture, the reported compressive-strength growth rate relative to ORCAS was 39.29% at 1 d and 20.39% at 28 d. For splitting tension, the 0.09 wt% mixture had a reported 58.22% increase at 1 d and 29.43% at 28 d. Flexural strength at 0.09 wt% also showed a stronger relative gain at early age than at 28 d. This does not mean that nanotubes cease to function later; rather, the control concrete itself becomes denser as hydration proceeds, reducing the relative margin available for nano-filling and nucleation to produce a percentage improvement.

Early-age enhancement is particularly relevant for shotcrete because tunnel and mine support often requires rapid development of load-bearing capacity. A material that gains strength quickly can shorten the period during which the freshly supported ground remains vulnerable. Nevertheless, early strength should not be pursued without checking long-term stability. The high-dosage 0.15 wt% mixture illustrates this point: its 1 d splitting response was slightly above control, but its 7 and 28 d splitting strengths fell below control. A short early-age screening program would therefore be insufficient to identify a robust dosage.

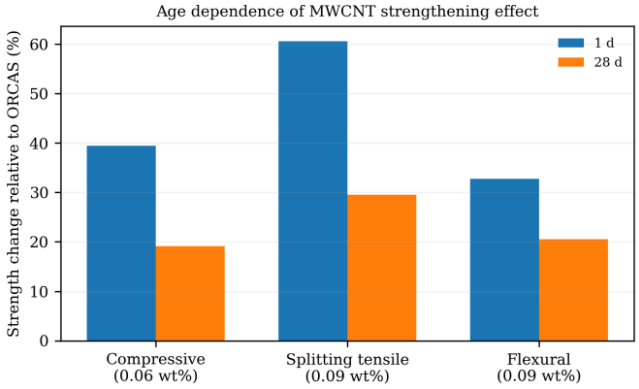


Figure 3. Relative early- and later-age strength changes reconstructed from the data in Li et al. [1].

5. MWCNT Microstructure, Pore Refinement and ITZ Mechanisms

5.1. Spatial Distribution and Agglomeration

Li et al. [1] used X-ray CT, equal-volume segmentation and three-dimensional coordinate extraction to characterize the spatial distribution of MWCNTs. The detected nanotube-count distribution followed a log-normal form for all mixtures, but the quality and uniformity of dispersion changed with dosage. Mixtures with 0.03, 0.06 and 0.09 wt% showed relatively concentrated and regular distributions, whereas 0.12 and 0.15 wt% produced more scattered patterns and lower goodness of fit. The source study linked this deterioration to increased nanotube agglomeration and to disturbance introduced by the shotcrete rebound process.

This observation is central to the interpretation of strength results. A nanomaterial can only reinforce the cementitious phase effectively when it is spatially available at the locations where pores and microcracks develop. An agglomerate may contain many nanotubes, yet it reduces effective reinforcement area because a large fraction of the nanotube surface is locked inside the cluster. It can also locally increase water demand and interrupt the continuity of hydration products. The relevant design variable is therefore not nominal dosage alone but dispersed, mechanically active dosage.

5.2. Pore Structure and Hydration Products

Mercury-intrusion results provide quantitative support for the densification mechanism. The control ORCAS had a total pore volume of 0.102 ml/g, an average pore diameter of 153 nm, a most probable pore size of 264 nm and a porosity of 25.2%. At 0.06 wt% MWCNT, these values decreased to 0.047 ml/g, 21 nm, 18 nm and 11.6%, respectively. At 0.09 wt%, the average pore diameter fell further to 17 nm and the most probable pore size to 9 nm, although total porosity was 13.7%. The authors reported reductions in harmful and more-harmful pore content of 30.4% and 52.5% for the 0.06 and 0.09 wt% mixtures, respectively [1].

The pore data show why a single property cannot define the optimum dosage. The 0.09 wt% mixture has the finest characteristic pore size, which is favorable for tensile and flexural resistance, but the 0.06 wt% mixture has the lowest total porosity and highest compressive strength. This indicates that pore-size refinement, total porosity, nanotube connectivity and local agglomeration influence different failure modes in different proportions. The mechanical optimum therefore emerges from a balance rather than from one microstructural indicator.

XRD analysis in the same study showed that MW-RCAS and ORCAS contained the same main hydration products, but the modified mixtures exhibited stronger characteristic peaks associated with hydration products such as C-S-H, CH and AFt. The 0.06 wt% mixture showed particularly strong C-S-H and CH signatures. The proposed mechanism is that well-dispersed MWCNTs provide nucleation sites and additional contact area, which accelerates hydration and fills microvoids in both the new matrix and the complex old-mortar/new-mortar interfaces around recycled aggregate.

5.3. Dosage-dependent Reinforcement Mechanisms

The mechanism summarized by Li et al. [1] can be interpreted as four dosage-dependent stages. In the nano-filling stage, a small amount of nanotubes occupies microvoids and supports the formation of additional hydration products. In the crack-bridging stage, a sufficiently connected nanotube network spans microcracks and stabilizes local stress transfer. In the pull-out-enhancement stage, somewhat higher nanotube content increases frictional and interfacial energy dissipation during crack opening, which is especially beneficial to splitting-tensile and flexural strength. Finally, in the agglomerate-nucleation stage, excessive nanotube content creates clusters that increase structural defects and cause a net reduction in mechanical performance.

The four-stage description is more useful for engineering design than a single optimum number because it explains how an optimum may shift when the performance objective changes. A mixture designed for maximum early compressive strength may reasonably target the crack-bridging region near 0.06 wt%, whereas a mixture designed for tensile or flexural response may move toward the pull-out-enhancement region near 0.09 wt%. What should be avoided is crossing into the agglomeration-dominated regime without simultaneously changing the dispersion technology.

5.4. Coupling of Nanostructure, Age and Macroscopic Strength

5.4.1. Normalized Pore-Structure Evolution with MWCNT Dosage

The pore-structure data provide one of the clearest quantitative bridges between microstructure and strength. Relative to ORCAS, total pore volume decreased from 0.102 ml/g to 0.047 ml/g at 0.06 wt% MWCNT, while porosity fell from 25.2% to 11.6%. The average pore diameter fell from 153 nm to 21 nm. At 0.09 wt%, the average diameter decreased further to 17 nm and the most probable pore size reached only 9 nm, even though total porosity increased slightly to 13.7%. At 0.12 and 0.15 wt%, all four pore indicators reversed direction and moved back toward the control condition. This non-monotonic response closely parallels the strength-versus-dosage curves and supports the interpretation that dosage governs performance through the balance between dispersed nanotube action and agglomeration.

The normalized pore curves also reveal that pore size and total pore volume need not reach their optimum at the same dosage. The 0.06 wt% mixture had the lowest total porosity and highest compressive strength, whereas the 0.09 wt% mixture had the smallest characteristic pore sizes and highest splitting-tensile and flexural strengths. A plausible interpretation, consistent with the source paper, is that compressive strength is particularly sensitive to the overall defect volume and matrix compactness, while tensile and flexural behavior are more sensitive to crack-path continuity, local bridging and the population of large harmful pores. Thus, the relevant microstructural target depends on the mechanical function being optimized.

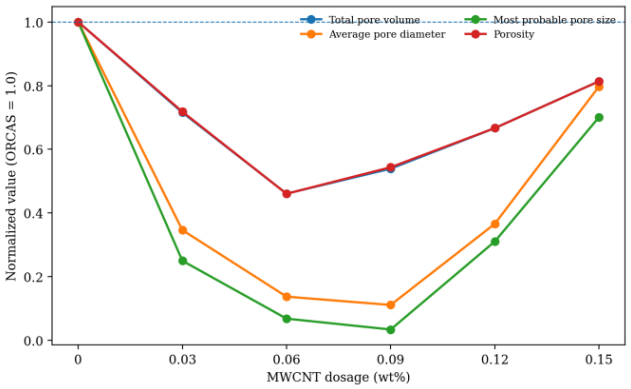


Figure 4. Normalized pore-structure parameters reconstructed from Li et al. [1]. Values below 1 indicate refinement relative to ORCAS.

5.4.2. Spatial Distribution as a Hidden State Variable

The CT-based distribution analysis reported by Li et al. [1] provides additional evidence that nominal dosage is an incomplete descriptor. For the 0.03, 0.06 and 0.09 wt% mixtures, the fitted log-normal distributions of detected nanotube-rich features had R2 values of 0.983, 0.995 and 0.953, respectively. At 0.12 and 0.15 wt%, the corresponding R2 values fell to 0.909 and 0.843, and the distribution width increased substantially. The number of detected features also did not increase proportionally with dosage; the 0.15 wt% mixture contained fewer detected features than the 0.12 wt% mixture. This is consistent with a transition from numerous dispersed features to larger agglomerates that are counted as fewer spatial objects.

For mixture design, the implication is significant: a dosage

specification should ideally be accompanied by a dispersion-quality requirement. Two mixtures containing 0.09 wt% MWCNT could behave differently if one is produced by controlled ultrasonic dispersion and the other by ordinary mixing. In laboratory research, CT statistics, image-based cluster size, electrical resistivity or another reproducible metric could be used as a state variable. In field production, a simpler surrogate may be needed, but the principle remains the same. The active reinforcement is the dispersed nanotube network, not the mass of nanotube powder added to the mixer.

5.4.3. Age-dependent Efficiency and Early Support Demand

The relative mechanical benefit of MWCNTs was strongest at early age. For the 0.06 wt% mixture, compressive strength increased from 5.99 MPa in ORCAS to 8.35 MPa at 1 d, a reported improvement of 39.29%. At 28 d, the corresponding increase was from 32.11 to 38.25 MPa, or 20.39%. The 0.09 wt% mixture increased 1 d splitting-tensile strength from 0.33 to 0.53 MPa, a reported increase of 58.22%, while the 28 d increase was 29.43%. This reduction in relative gain with age is consistent with the progressive hydration of the control matrix: as ordinary RCAS becomes denser with curing, the proportional advantage supplied by nucleation and nano-filling naturally decreases.

For underground support, early-age performance has a structural meaning that differs from ordinary cast concrete. Shotcrete may be required to stabilize freshly excavated ground within hours or days, before a conventional lining is installed. A material modification that accelerates the development of compressive and tensile resistance can therefore improve the safety margin during the period of highest ground relaxation. At the same time, the early-age data should not be used alone to choose dosage. The 0.15 wt% mixture illustrates why: although some 1 d tensile indicators were close to or above the control, later-age strength deteriorated as agglomeration and associated defects dominated the response.

An appropriate experimental program should consequently evaluate at least one early age and one mature age, and should track both absolute strength and relative improvement. For RCAS intended for rapid support, the design objective may be multi-objective: maximize 1-3 d load capacity while maintaining 28 d strength, pumpability and durability. The source results suggest that the 0.06-0.09 wt% range can satisfy this balance more effectively than a single high dosage intended to maximize one early result.

5.4.4. Interpreting ITZ Densification in Recycled Particles

In recycled aggregate concrete, ITZ improvement has a compound meaning because at least two generations of interface can coexist. The old ITZ lies between original natural aggregate and adhered old mortar, while the new ITZ forms around the recycled particle in the new matrix. Cracks may follow either region depending on local stiffness, porosity and bond. The SEM and XRD observations in Li et al. [1] indicate that suitably dispersed MWCNTs can fill microvoids, provide nucleation surfaces and increase the amount of hydration products in the new matrix and around recycled-particle interfaces. This does not remove the old ITZ, but it can reduce the continuity of weak paths across the composite particle-matrix system.

The ITZ interpretation also helps explain why tensile properties can continue to improve at a dosage slightly above the compressive optimum. Tensile fracture is governed by the weakest connected crack path rather than by average matrix density alone. If additional dispersed nanotubes bridge or interrupt the most critical interface-scale microcracks, the splitting or flexural strength may still rise even when overall porosity has already reached its minimum. Once agglomeration develops, however, clusters introduce new weak zones and reconnect the crack path, causing both tensile and compressive performance to decline.

6. Steel-Fiber-Reinforced Shotcrete: Tensile Response and Toughness

6.1. Uniaxial Tensile Behavior and Failure Stages

Zhang et al. [2] divided the SFRCAS uniaxial tensile stress-strain curve into three stages: an ascending branch before peak stress, a descending branch from peak stress toward residual stress, and a relatively smooth residual stage. This three-stage pattern is a direct expression of progressive cracking. Before the peak, distributed microcracks grow while the matrix and fibers share load. Around the peak, one or several cracks localize and the load drops. After localization, fibers crossing the crack are progressively pulled out and the remaining aggregate interlock and friction sustain a residual tensile stress.

The distinction between peak strength and post-peak resistance is critical for shotcrete support. Peak tensile strength controls crack initiation, but underground support is rarely allowed to be judged only by first cracking. Ground movement, joint opening and local impact can impose deformation after a crack has formed. Steel fibers provide a mechanism for maintaining integrity under this deformation by transferring tensile force across the crack opening. The source study reported audible fiber pull-out during the residual stage, confirming that pull-out rather than widespread fiber rupture dominated the post-peak mechanism.

Without steel fibers, the C30R50F0 mixture exhibited brittle fracture and did not develop a conventional descending branch. Adding fibers changed both the rising and descending portions of the curve. As fiber volume fraction increased, the ascending branch became steeper, peak stress and strain increased, and the post-peak response became more stable. This behavior contrasts with MWCNT modification, which acts mainly at the microcrack and matrix scale; steel fibers become especially active after cracking has localized to a scale comparable with the fiber length.

6.2. Effect of Recycled Aggregate Replacement

Direct-tension experiments on steel-fiber-reinforced recycled fine aggregate concrete also distinguish axial tension from splitting tension and document the influence of fiber geometry [28].

At constant C30 strength grade and 1% steel-fiber volume fraction, increasing recycled aggregate replacement from 0% to 100% reduced the uniaxial tensile strength from 2.6 to 2.2 MPa and the tensile elastic modulus from 39.4 to 33.0 GPa. At the same time, peak tensile strain increased from 148.8 to 222.7 microstrain. The source paper attributed these trends to the higher porosity and crushing index of recycled aggregate and to the larger and weaker ITZ population. Under tension, cracks preferentially propagate through or near these weak zones, reducing stiffness and peak stress but allowing larger deformation before and around localization [2].

The energy indicators do not vary monotonically with

replacement ratio. Tensile work W0.2 increased from 5117.25 N·mm at 0% replacement to 6305.26 N·mm at 70%, then fell to 4791.17 N·mm at 100%. The tensile toughness ratio similarly increased from 0.15 to 0.21 at 70% and then fell to 0.16 at full replacement. This result suggests that a moderate-to-high proportion of recycled aggregate can increase deformation-related energy dissipation when an effective fiber-bridging network is present, even though strength and modulus decline. At full replacement, however, the accumulated weakness of the aggregate/ITZ system becomes sufficiently severe to reduce the useful energy capacity.

This strength-toughness trade-off is important for support design. A specification based only on compressive strength or elastic modulus could incorrectly classify all increases in recycled aggregate content as undesirable. For deformation-tolerant shotcrete, a controlled reduction in stiffness accompanied by increased tensile strain capacity may be beneficial, provided that peak load capacity and durability remain above project requirements. The 70% replacement result in the source study should therefore be understood as an observed optimum within that test matrix, not as a universal replacement recommendation.

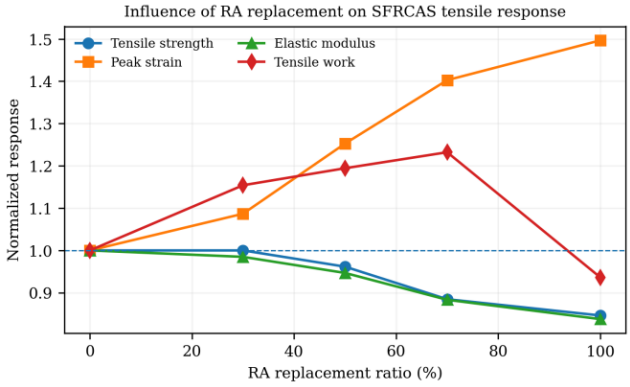


Figure 5. Normalized tensile-response indicators for the recycled-aggregate replacement series, reconstructed from Zhang et al. [2].

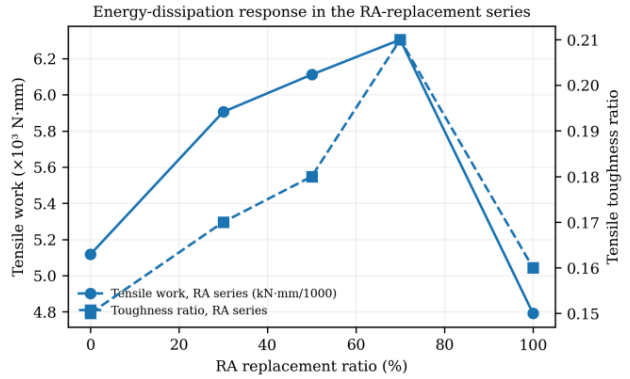


Figure 6. Tensile work and toughness ratio versus recycled-aggregate replacement ratio, reconstructed from Zhang et al. [2].

6.3. Effect of Steel-Fiber Volume Fraction

The steel-fiber series provides the clearest evidence of crack-bridging effectiveness. At C30 and 50% recycled aggregate replacement, increasing the fiber volume fraction from 0% to 2% raised uniaxial tensile strength from 1.5 to 3.3 MPa, an increase of 120% reported by Zhang et al. [2]. Peak tensile strain increased from 130 to 243 microstrain and tensile elastic modulus increased from 34.7 to 50.7 GPa. For mixtures with measurable post-peak energy, W0.2 increased from 2680.34 N·mm at 0.5% fiber to 8718.33 N·mm at 2% fiber.

The improvement is not simply a result of adding a high-strength material to the mixture. Steel fibers are effective because their geometry allows stress to be transmitted across cracks by bond and mechanical anchorage. Hooked ends increase pull-out resistance, while multiple randomly distributed fibers reduce the probability that a single crack can propagate through the entire section without encountering reinforcement. As fiber content rises, the crack-bridging network becomes denser, which increases both peak stress and the energy required for crack opening and fiber pull-out.

The source data also show that steel fibers can compensate for part of the performance loss caused by recycled aggregate. This compensation has practical significance because it expands the usable recycled-aggregate content without requiring the matrix itself to match the stiffness of natural-aggregate shotcrete. However, the higher fiber content that improves hardened performance can also reduce workability. Hence, the engineering optimum should be found by jointly considering pumpability, rebound, fiber orientation, tensile performance and cost rather than maximizing fiber content without constraint.

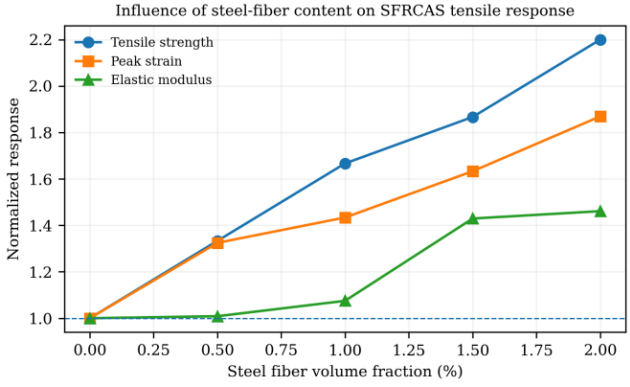


Figure 7. Normalized effect of steel-fiber volume fraction on tensile strength, peak strain and elastic modulus, reconstructed from Zhang et al. [2].

Table 4. Selected tensile-property changes reported by Zhang et al. [2].

Series change	Tensile strength	Peak strain	Elastic modulus
RA 0% -> 100%	2.6 -> 2.2 MPa	148.8 -> 222.7 microstrain	39.4 -> 33.0 GPa
SF 0% -> 2%	1.5 -> 3.3 MPa	130 -> 243 microstrain	34.7 -> 50.7 GPa
C20 -> C40 (r=50%, Vf=1%)	1.7 -> 3.0 MPa	140.1 -> 208.5 microstrain	29.8 -> 42.3 GPa

6.4. Effect of Concrete Strength Grade

At 50% recycled aggregate replacement and 1% steel fiber, increasing the concrete strength grade from C20 to C40 increased uniaxial tensile strength from 1.7 to 3.0 MPa and elastic modulus from 29.8 to 42.3 GPa. Peak strain also increased, from 140.1 to 208.5 microstrain, while tensile work rose from 3807.26 to 8218.75 N·mm. The authors found that the tensile-to-prismatic-compressive strength ratio remained approximately 0.07, indicating that the increase in matrix strength improved compressive and tensile capacity in a broadly coordinated way [2].

Higher matrix strength strengthens the bond that anchors fibers and aggregates, so it can increase both peak load and the amount of energy transferred into fiber pull-out. At the

same time, a strong matrix can make the immediate post-peak drop steeper if there is insufficient bridging reinforcement, because stored elastic energy is released rapidly when a dominant crack forms. This again reinforces the value of evaluating full stress-strain behavior rather than a single strength number.

6.5. Tensile Work, Deformability and Parameter Sensitivity

6.5.1. Strength-grade Sensitivity

The strength-grade series in Zhang et al. [2] demonstrates that matrix quality affects not only peak tensile stress but the entire deformation-energy response. With recycled aggregate replacement fixed at 50% and steel-fiber volume fraction at 1%, increasing the concrete grade from C20 to C30 raised tensile strength from 1.7 to 2.5 MPa, peak tensile strain from 140.1 to 186.4 microstrain, tensile modulus from 29.8 to 37.3 GPa and tensile work from 3807.26 to 6111.85 N·mm. Increasing the grade further to C40 raised the same values to 3.0 MPa, 208.5 microstrain, 42.3 GPa and 8218.75 N·mm. Thus, stronger matrices did not simply become more brittle within this fiber-reinforced series; the combination of improved matrix cohesion and fiber anchorage increased both resistance and energy absorption.

The tensile-to-prismatic-compressive strength ratio remained near 0.07 across the strength-grade series. This stability is useful because it suggests that, for the tested material family, changes in matrix strength influenced compression and direct tension in a broadly coordinated way when the recycled aggregate and fiber contents were fixed. Nevertheless, the ratio should not be treated as universal for all RCAS because aggregate quality, fiber orientation, spray direction and test geometry can alter tensile behavior more strongly than compressive behavior.

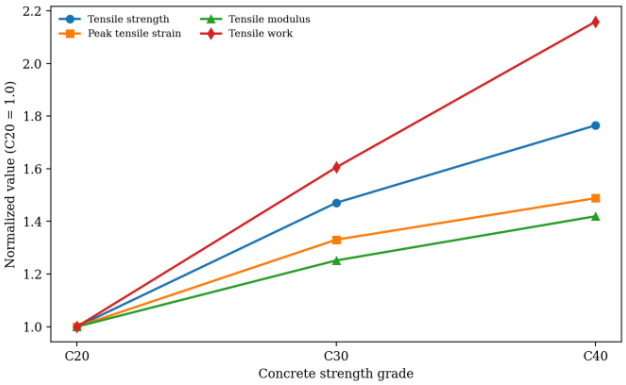


Figure 8. Normalized effect of concrete strength grade on tensile response reconstructed from Zhang et al. [2].

6.5.2. Recycled Aggregate Replacement: Stiffness Loss Versus Deformability

The recycled-aggregate series shows a characteristic trade-off. Tensile strength was essentially unchanged between 0% and 30% replacement at 2.6 MPa, but then decreased to 2.5, 2.3 and 2.2 MPa at 50%, 70% and 100%. In contrast, peak tensile strain increased from 148.8 microstrain at 0% replacement to 161.7, 186.4, 208.7 and 222.7 microstrain. Tensile modulus decreased from 39.4 GPa to 33.0 GPa over the same range. Mechanically, the recycled aggregate introduces more compliant and porous phases, so the composite deforms more under a given stress while local weak interfaces reduce the stress level at which a dominant crack forms.

This response is relevant to support systems that must accommodate ground deformation. A lower modulus can reduce stress concentration under imposed displacement, and higher tensile strain capacity can delay abrupt loss of integrity. However, these potential advantages cannot be considered independently of reduced peak strength and durability. The correct engineering question is therefore not whether high recycled content is intrinsically good or bad, but whether a given replacement level produces an acceptable balance between resistance, deformability, energy dissipation and service-life requirements for the intended support environment.

Table 5. Direct-tension indicators for the recycled-aggregate replacement series reported by Zhang et al. [2].

RA replacement	ft (MPa)	Peak strain (microstrain)	Et (GPa)	W0.2 (N mm)	Re,0.2
0%	2.6	148.8	39.4	5117.25	0.15
30%	2.6	161.7	38.8	5905.60	0.17
50%	2.5	186.4	37.3	6111.85	0.18
70%	2.3	208.7	34.8	6305.26	0.21
100%	2.2	222.7	33.0	4791.17	0.16

6.5.3. Fiber Fraction And the Transition from Brittle to Bridged Fracture

The fiber-volume series provides a direct view of the transition from brittle matrix fracture to a bridged cracking process. The fiber-free C30R50F0 specimen reached only 1.5 MPa tensile strength and approximately 130 microstrain at peak; the source study reported brittle fracture without a complete descending branch suitable for the same tensile-work calculation. At 0.5% fiber, tensile strength increased to 2.0 MPa, and measurable post-peak energy appeared. At 1%, 1.5% and 2%, tensile strength increased to 2.5, 2.8 and 3.3 MPa, while peak strain reached 186.4, 212.3 and 243 microstrain, respectively.

The evolution of tensile work is even more striking. W0.2 increased from 2680.34 N·mm at 0.5% fiber to 6111.85 N·mm at 1%, 7572.85 N·mm at 1.5% and 8718.33 N·mm at 2%. The corresponding toughness ratio increased from 0.10 to 0.18 and then approximately plateaued at 0.20 for 1.5-2%. This pattern suggests diminishing returns in a normalized toughness measure even while absolute energy absorption continues to grow. From a design perspective, the distinction matters: a higher fiber fraction can continue to add energy capacity, but the efficiency gained per additional unit of fiber may decline.

The source paper attributed the improvement to fiber bridging, pull-out resistance and the development of a three-

dimensional reinforcement network. At very low fiber content, the spacing between effective fibers is large and some cracks can localize without intersecting enough reinforcement. As volume fraction increases, the probability of crack-fiber intersection rises and the load carried by the matrix can be progressively transferred to multiple fibers. At still higher content, workability and dispersion become limiting; bundled fibers or preferential orientation can reduce the effective reinforcement fraction even when the nominal fiber mass continues to increase.

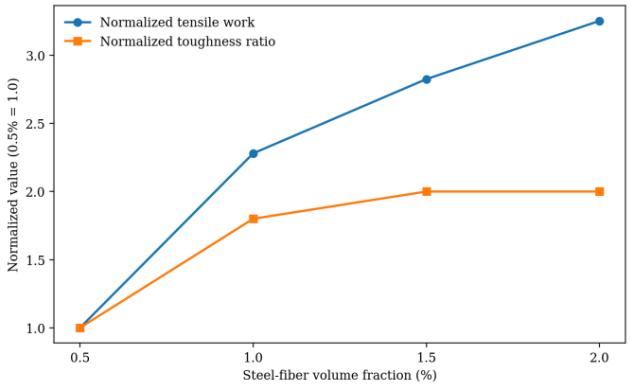


Figure 9. Normalized tensile work and toughness ratio for the steel-fiber series, reconstructed from Zhang et al. [2].

6.5.4. Practical Interpretation of Tensile Work and Residual Response

Tensile strength is a peak quantity, whereas tensile work integrates the load carried through deformation. In a support lining subjected to convergence, local blasting disturbance or joint opening, the ability to continue carrying load after first cracking can be as important as the first-crack stress. The three-stage tensile curves reported by Zhang et al. [2] therefore provide a more structurally meaningful description than peak strength alone. The descending branch reflects the competition between crack localization and fiber pull-out; the residual stage reflects friction, aggregate interlock and continuing fiber bridging after the main crack has formed.

The non-monotonic toughness response with recycled aggregate content also becomes easier to understand in this energy framework. Increasing recycled aggregate introduces weaker interfaces and can enlarge deformation before localization, which increases the displacement over which fibers can perform pull-out work. Up to a certain level, this can raise tensile work despite lower peak strength. At full replacement in the source study, however, the weak matrix/ITZ network reduced the load carried during this deformation enough that total tensile work fell. The optimum is therefore governed by the area under the curve, not by either peak stress or peak strain considered separately.

7. Constitutive Interpretation and Multi-Scale Mix Design

Constitutive relationships are necessary when tensile test data are incorporated into numerical analyses of sprayed-concrete support. Zhang et al. [2] expressed tensile stress and strain relative to their respective peak values and compared the segmented Guo description with a single-parameter Sargin formulation. Because the ascending and descending branches can be shaped independently, the Guo relation represented the reported normalized response more closely. The two normalized variables used for this comparison are defined below. Comparable studies of fully recycled aggregate concrete show that constituent composition can also modify the shape of the stress–strain curve, although compressive and tensile constitutive parameters must not be transferred indiscriminately [29].

$$x = \frac{\varepsilon}{\varepsilon_t}, \qquad y = \frac{\sigma}{\sigma_t} \tag{2}$$

Where x and y are normalized tensile strain and stress, respectively; ε and σ denote axial tensile strain and stress; and ε_t and σ_t are their corresponding peak values. Both variables are dimensionless.

In the segmented formulation discussed by Zhang et al. [2], the ascending-branch parameter describes pre-peak curve shape, while the descending-branch parameter governs post-peak softening. The reported trends with recycled aggregate replacement and steel-fiber fraction are consistent with changes in composite stiffness, crack localization and fiber bridging. However, the lower goodness of fit reported for the descending parameter indicates that a single macroscopic parameter cannot uniquely capture fiber orientation, pull-out resistance and interfacial heterogeneity. Consequently, the original fitted relations should be used only within their stated experimental domain rather than treated as universally calibrated material constants.

Two implications follow for engineering modelling. First, changing recycled aggregate content or fiber dosage affects not only the peak strength but also peak strain, stiffness and post-peak work. Second, a constitutive curve inferred from aggregate response indicators requires independent validation against a complete stress–strain history before it can be used to predict crack widths or support displacements. More detailed microstructure-informed experiments, including in-situ CT studies of steel-fiber-reinforced recycled concrete, provide a way to connect crack development and parameter selection [25].

The MWCNT experiment [1] did not establish a complete direct-tension constitutive law for the modified shotcrete. Its pore refinement and ITZ observations nevertheless suggest a potential route for increasing crack-initiation resistance and matrix integrity. Fiber–matrix bond investigations using nanoparticle-modified cement paste also indicate that nanoparticle dosage and fiber geometry can interact, although those findings do not establish a combined optimum for recycled shotcrete [26]. Thus, the proposed division between nano-scale matrix strengthening and macro-scale bridging remains a testable hypothesis rather than a measured hybrid response.

7.1. Nano-scale Versus Fiber-Scale Reinforcement Mechanisms

7.1.1. Different Scales, Different Functions

The most important result of the comparison is that MWCNTs and steel fibers solve different parts of the recycled-shotcrete problem. MWCNTs operate at nano-to-microscale. Their main reported functions are filling small pores, promoting hydration, densifying the ITZ, bridging microcracks and increasing the energy required for microcrack growth [1]. Steel fibers operate at millimeter-to-centimeter scale. Their key function is to bridge an already localized crack, provide pull-out resistance and stabilize the post-peak response [2]. Treating the two reinforcements as direct substitutes therefore misses the scale separation in their mechanisms.

The recycled aggregate itself creates defects over multiple

scales. Old mortar contains capillary pores and microcracks; the interface between old aggregate and old mortar may be weak; a new ITZ forms between recycled aggregate and new mortar; and stress concentration can link these local defects into a macrocrack. A rational strengthening system should therefore interrupt the damage cascade at more than one stage. Nano-reinforcement can reduce the probability that a local defect develops into a critical crack, while steel fibers can prevent a critical crack from producing sudden loss of load-carrying capacity.

This interpretation also explains why the optimum MWCNT dosage is narrow while the steel-fiber response in the tested range is more monotonic. Nanotube efficiency depends on dispersion at a scale where interparticle attraction is intense; adding more nanotubes eventually reduces the effective reinforced volume because agglomerates form. Steel fibers are much larger and mechanically discrete, so increasing their fraction from 0% to 2% continued to increase the number of crack bridges in Zhang et al.'s test matrix. At still higher fiber contents, however, workability, orientation and balling would also be expected to impose an upper practical limit.

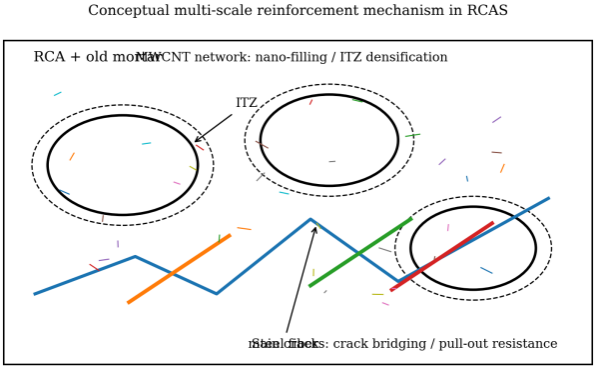


Figure 10. Conceptual multi-scale reinforcement mechanism synthesized from the microstructural observations in Ref. [1] and the uniaxial tensile behavior in Ref. [2].

7.1.2. Strength, Deformability and Energy Dissipation

The normalized data show that performance improvement is multidimensional. MWCNTs can increase compressive, splitting-tensile and flexural strength, but the best dosage depends on the failure mode and age. Recycled aggregate replacement in fiber-reinforced shotcrete can reduce tensile strength and stiffness while increasing peak strain. Steel fibers can then raise strength, strain capacity and tensile work simultaneously. A mixture that is strongest in compression is therefore not automatically the mixture with the best tensile energy dissipation, and a mixture with the highest stiffness is not automatically the most deformation-tolerant support material.

For underground support, this distinction matters because the loading environment can evolve. Immediately after excavation, early compressive and bond strength are important for stabilizing the exposed ground. During later ground convergence, joint movement or dynamic disturbance, tensile strain capacity and post-crack energy dissipation become more important. The source studies suggest a possible staged design philosophy: use matrix-scale modification to secure early integrity and ITZ quality, and use fibers to preserve residual capacity under larger deformation.

Such a philosophy should not be interpreted as a recommendation to combine the exact optimum dosages from the two source studies. The 0.06-0.09 wt% MWCNT range was obtained under one dispersion process and one recycled aggregate source, while the 1-2% fiber range was evaluated under another mixture system. A hybrid mixture could alter viscosity, entrained air, rebound, fiber orientation and nanotube distribution. The combined optimum must therefore be determined experimentally rather than by simply superimposing two independent optima.

7.1.3. Proposed Hybrid Design Hypothesis

A testable hybrid hypothesis can nevertheless be formulated. In a well-dispersed system, a low MWCNT dosage could be used to reduce matrix and ITZ porosity, while a moderate steel-fiber fraction could provide macrocrack bridging. If the nano-modification raises the local bond quality around the fiber and recycled aggregate, fiber pull-out may require more energy; conversely, if excessive MWCNTs increase viscosity or agglomeration, fiber distribution may become less uniform and the hybrid response could deteriorate. The interaction is therefore potentially synergistic but not guaranteed.

A suitable hybrid experimental matrix would vary at least three factors: recycled aggregate quality/replacement ratio, MWCNT dosage around the beneficial window, and steel-fiber volume fraction. Fresh-state rheology, pumping pressure, rebound, fiber orientation and nanotube dispersion should be measured alongside compressive and tensile properties. Full tensile or flexural fracture curves are needed to distinguish matrix strengthening from post-crack bridging. Micro-CT and SEM could then be used to determine whether improved macro-scale toughness is actually associated with denser fiber-ITZ regions and a more uniform nanotube network.

Table 6. Mechanism-based design interpretation derived from the two source studies.

Design issue	Most relevant mechanism	Main caution
Early matrix strength	MWCNT nano-filling + hydration promotion	Agglomeration at excessive dosage
ITZ quality	MWCNT pore refinement / microcrack bridging	Depends on dispersion and RCA moisture state
Peak tensile capacity	Matrix quality + fiber bridging	RA weak interfaces can reduce peak stress
Post-crack toughness	Steel-fiber pull-out and anchorage	Workability, orientation and rebound
High recycled content	Fiber compensation + controlled ITZ	Durability and long-term field validation required

7.2. Mechanism-Based Mixture Design Procedure

Step 1: Characterize recycled aggregates before selecting replacement

A rational RCAS design should begin with the recycled aggregate rather than with the desired replacement percentage. Apparent density, bulk density, water absorption, crushing value, grading and, where possible, adhered-mortar content should be measured first. The two source studies demonstrate why this is necessary: their recycled aggregates differed substantially in absorption and crushing resistance even

though both were produced from waste concrete. A replacement ratio therefore has no unique mechanical meaning unless aggregate quality is known.

For field production, moisture conditioning should be linked to absorption. The objective is not necessarily complete saturation, but a repeatable moisture state that prevents uncontrolled water exchange during batching and pumping. Trial mixtures should be evaluated for slump or rheological parameters after the same waiting period expected on site, because recycled aggregate can continue absorbing water after initial mixing. This step stabilizes the effective water-binder ratio and makes subsequent reinforcement optimization more reproducible.

Step 2: Define the performance function of reinforcement

The next step is to decide which deficiency is controlling the design. If the main limitation is early matrix strength, high porosity or weak ITZ quality, the MWCNT study indicates that a low-dose, well-dispersed nano-modification can be effective. If the main limitation is brittle tensile fracture or insufficient post-crack capacity, the steel-fiber study indicates that hooked fibers provide a direct bridging mechanism. When both problems are important, a hybrid design can be justified conceptually, but the two dosages should not be selected independently because both modifications influence water demand, flow and particle interactions.

This function-based approach avoids the common mistake of selecting an additive because it improved one property in another cement-based system. Shotcrete has a distinctive placement process: particles are accelerated, impact the receiving surface, and may rebound; fibers can orient during pumping and spraying; nanomaterials can alter viscosity and yield stress. The reinforcement must therefore be evaluated within the full process route, from mixing through pumping to the in-place sprayed layer.

Step 3: Optimize constructability and hardened properties together

Li et al. [1] observed that increasing MWCNT dosage reduced slump while increasing relative yield stress and plastic viscosity. Zhang et al. [2] likewise reported lower slump as steel-fiber fraction increased: in the C30, 50% recycled-aggregate series, slump fell from 116 mm without fiber to 64 mm at 2% fiber. These results show that mechanical enhancement consumes part of the fresh-state workability margin. An optimization that ignores pumping or sprayability can therefore produce a laboratory mixture that cannot be delivered uniformly in practice.

A useful design sequence is to define an acceptable fresh-state window first, then search for the reinforcement combination that maximizes the required hardened indicators within that window. Rebound rate and in-place composition should be monitored because the material retained on the surface can differ from the batched material. In fiber shotcrete, this is especially important because preferential rebound of coarse particles or fibers changes the local fiber volume fraction and aggregate grading. For nanomodified shotcrete, pump shear and accelerator addition may change dispersion after the laboratory suspension has been prepared.

Step 4: Verify matrix/ITZ quality and tensile response

Compressive strength alone is insufficient for validating RCAS intended for support. The MWCNT study demonstrates that compressive, splitting-tensile and flexural optima do not occur at exactly the same dosage, while the SFRCAS study demonstrates that strength, modulus, strain and energy can move in different directions as recycled aggregate content changes. A minimum verification set should therefore include one matrix-dominated indicator, one direct or indirect tensile indicator and one post-crack or energy indicator. Where resources permit, pore structure or microscopic examination should be used to confirm that the intended mechanism is actually present.

For numerical applications, the complete tensile stress-strain curve is especially valuable. Peak stress and modulus control the pre-crack stiffness and onset of damage, while the descending and residual branches determine how a cracked support redistributes load. The empirical constitutive models fitted by Zhang et al. [2] provide a starting point, but field calibration should consider spray-direction anisotropy, fiber orientation and the actual recycled aggregate used in the project.

Step 5: Iterate toward an engineering rather than laboratory optimum

The final optimum should be defined by project constraints. A tunnel primary support mixture may prioritize early strength and deformation capacity; a repair layer may prioritize bond, durability and crack control; a mine roadway may place greater emphasis on impact resistance and residual toughness. Material cost, embodied energy, mixing complexity and quality-control requirements should also be considered. This is particularly relevant for MWCNTs, where a small mass fraction can require a nontrivial dispersion process, and for steel fibers, where higher volume fractions increase material consumption and handling demands.

The workflow proposed here is therefore iterative. Recycled aggregate quality establishes the baseline; fresh-state tests define a constructability envelope; reinforcement is selected by mechanism; hardened matrix and tensile tests confirm performance; and full-scale spraying validates the in-place material. The objective is not to maximize any single laboratory number but to produce a mixture whose actual sprayed state satisfies the structural and construction functions simultaneously.

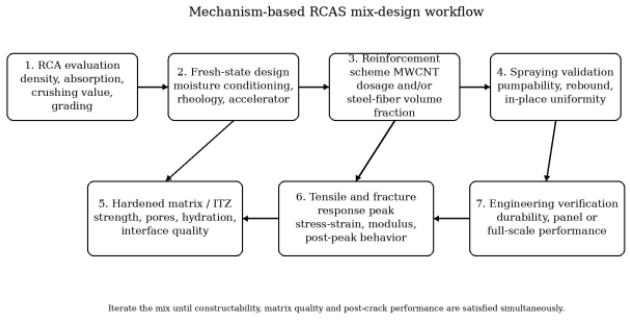


Figure 11. Proposed mechanism-based design workflow synthesized from the two source studies. The workflow is a design proposal of the present paper, not a directly tested result.

7.3. Engineering Applications and Sustainability

RCAS is particularly attractive for underground and repair applications because demolished concrete is often available near urban infrastructure projects and because shotcrete can be placed without conventional formwork. The source studies demonstrate that the mechanical limitations of recycled aggregate are not immutable. Matrix-scale modification can recover or exceed control strength, while steel fibers can significantly increase tensile capacity and post-crack energy absorption. This broadens the range of applications in which recycled coarse aggregate can be considered without

assuming that high replacement necessarily produces brittle, low-performance support.

However, sustainability should not be inferred from recycled-content percentage alone. MWCNT production is energy intensive, steel fibers add material and processing impacts, and poor workability can increase rebound and waste. A mixture with higher recycled aggregate content but excessive rebound may consume more binder and generate more overspray than a better-balanced mixture. Future engineering evaluation should therefore couple mechanical performance with a life-cycle inventory that includes aggregate processing, transport, nanomaterial or fiber production, pumping energy, rebound loss, repair frequency and service life.

Construction control is equally important. Recycled aggregate moisture conditioning should be standardized so that effective water content remains stable. MWCNT dispersion should be verified rather than assumed from mixing time, and field mixing equipment must reproduce the energy input used in laboratory dispersion. Steel-fiber content should be checked in sprayed panels because rebound can change the in-place fiber fraction and orientation relative to the batched mixture. Core or panel sampling after spraying remains essential for confirming that the in-place material matches the design assumptions.

For numerical design, the tensile constitutive relationships from Zhang et al. [2] provide a useful foundation, but implementation should account for field variability. The local fiber orientation in a sprayed layer, the anisotropy created by the spray direction, the distribution of recycled coarse aggregate and the quality of substrate bond can all affect structural response. A constitutive law calibrated on laboratory specimens should therefore be validated against panel tests, flexural toughness tests and, where possible, full-scale support elements before it is used for safety-critical design.

7.4. Limitations and Future Research

This work is a comparative analysis of two independently published experimental programs, not a new joint MWCNT–steel-fiber experimental campaign. The MWCNT series employed full recycled-coarse-aggregate replacement, whereas the steel-fiber series varied recycled aggregate replacement and used different aggregate properties, mixture designs, specimen dimensions and loading methods. Direct numerical pooling would therefore confound reinforcement type with these other variables. In addition, the source studies do not supply a common dataset for long-term durability, combined reinforcement dosage or full-scale structural response. The present design framework should be interpreted as a mechanism-based synthesis requiring targeted validation.

A second limitation is that the MWCNT study concentrated on static strength and microstructure, whereas the steel-fiber study concentrated on direct tensile behavior. Neither dataset alone provides a full picture of impact resistance, cyclic loading, fatigue, bond to rock, permeability, freeze-thaw resistance, chloride transport or long-term creep and shrinkage. These properties are especially relevant to underground infrastructure and repair, where water, repeated disturbance and sustained deformation can interact with the recycled-aggregate ITZ over long service periods.

Future research should therefore establish coupled performance maps rather than single-property optima. For nano-modified RCAS, dispersion quality should be quantified using reproducible indices such as CT-based spatial statistics, electrical response or image-derived agglomeration metrics. For fiber-reinforced RCAS, the in-place fiber orientation distribution should be measured after spraying and related to tensile softening. A combined program should include rheology and pumping pressure because the same modification that improves hardened performance may change sprayability and rebound.

The role of recycled aggregate quality also deserves more systematic treatment. The two source papers used aggregates with substantially different water absorption and crushing values. Separating recycled aggregate by attached mortar content, strength class or parent-concrete origin could allow performance to be predicted from measurable aggregate descriptors rather than from replacement percentage alone. Such classification is likely to be particularly valuable for shotcrete because particle rebound and pumping may selectively alter the grading and composition of the material that actually remains on the sprayed surface.

Finally, data-driven approaches could be useful once sufficiently large and standardized datasets are available. Inputs could include aggregate density, absorption, crushing index, adhered mortar fraction, binder composition, MWCNT dosage and dispersion index, fiber geometry and volume fraction, accelerator dosage, slump/rheology, spray pressure and curing age. Outputs could include rebound, compressive strength, tensile constitutive parameters, toughness and durability. Machine-learning models should not replace mechanism-based understanding, but they could help identify interaction effects and narrow the experimental search space for multi-factor RCAS optimization.

8. Conclusions

The comparison distinguishes two complementary reinforcement mechanisms in recycled coarse aggregate shotcrete. The following findings relate to the test conditions of the cited investigations, while the proposed joint reinforcement strategy remains to be verified experimentally:

(1) MWCNT modification exhibits a distinct dosage window. In Li et al. [1], 0.06 wt% produced the highest compressive strength, whereas approximately 0.09 wt% produced the strongest splitting-tensile and flexural response. Excessive dosage, particularly 0.15 wt%, caused agglomeration and reduced mechanical performance.

(2) The MWCNT benefit is strongly associated with dispersion, pore refinement, hydration promotion and ITZ densification. The 0.06-0.09 wt% mixtures markedly reduced characteristic pore sizes and harmful pore content, supporting the interpretation that matrix-scale defect control governs the strength increase.

(3) Increasing recycled aggregate replacement in SFRCAS reduced tensile strength and elastic modulus but increased peak tensile strain. Tensile work and toughness reached their highest values at an intermediate-to-high replacement ratio in the tested series, showing that deformation capacity and energy dissipation do not necessarily follow the same trend as peak strength.

(4) Steel fibers provided strong and largely monotonic tensile enhancement over the investigated 0-2% range. Increasing fiber fraction from 0% to 2% raised uniaxial tensile strength from 1.5 to 3.3 MPa and substantially increased peak strain and tensile work [2]. The mechanism is primarily crack bridging and pull-out resistance after microcracks have localized.

(5) The integrated experimental evidence supports a multi-scale design concept: nano-reinforcement is most suited to improving matrix/ITZ quality and delaying crack initiation, while steel fibers are most suited to controlling crack opening and preserving post-peak load transfer. A hybrid system could be promising, but the interaction between MWCNT dispersion, fiber distribution, workability and rebound must be validated experimentally rather than inferred by simply combining independent optimum dosages.

(6) Future RCAS design should evaluate fresh-state constructability, early strength, direct tensile constitutive behavior, energy dissipation and long-term durability together. Aggregate quality descriptors and in-place reinforcement distribution should be incorporated into design and quality control so that recycled content can be increased without sacrificing reliability.

References

[1] Li, P., Chen, L., Ma, H., et al. (2023). Spatial distribution characteristics and microscopic mechanisms for enhancing mechanical properties of MWCNTs in recycled coarse aggregate shotcrete. Construction and Building Materials, 364, 129927.

[2] Zhang, X., Ma, C., Liu, C., et al. (2024). Uniaxial tensile properties of steel fiber-reinforced recycled coarse aggregate shotcrete: Test and constitutive relationship. Construction and Building Materials, 411, 134202.

[3] Standardization Administration of China. (2010). Recycled Coarse Aggregate for Concrete: GB/T 25177—2010. Beijing.

[4] Ministry of Housing and Urban-Rural Development of China. (2019). Standard for Test Methods of Concrete Physical and Mechanical Properties: GB/T 50081—2019. China Architecture & Building Press.

[5] Ministry of Housing and Urban-Rural Development of China. (2015). Technical Code for Engineering of Ground Anchorages and Shotcrete Support: GB 50086—2015. China Planning Press.

[6] Ministry of Housing and Urban-Rural Development of China. (2016). Standard for Test Method of Performance on Ordinary Fresh Concrete: GB/T 50080—2016. China Architecture & Building Press.

[7] Ministry of Housing and Urban-Rural Development of China. (2016). Technical Specification for Application of Sprayed Concrete: JGJ/T 372—2016. China Architecture & Building Press.

[8] China Association for Engineering Construction Standardization. (2009). Standard Test Methods for Fiber Reinforced Concrete: CECS 13:2009. Beijing.

[9] Ministry of Water Resources of China. (2020). Test Code for Hydraulic Concrete: SL/T 352—2020. Beijing.

[10] Duarte, G., Bravo, M., de Brito, J., et al. (2019). Mechanical performance of shotcrete produced with recycled coarse aggregates from concrete. Construction and Building Materials, 210, 696–708.

[11] Nobre, J., Bravo, M., de Brito, J., et al. (2020). Durability performance of dry-mix shotcrete produced with coarse recycled concrete aggregates. Journal of Building Engineering, 29, 101135.

[12] Tam, V. W. Y., Soomro, M., & Evangelista, A. C. J. (2018). A review of recycled aggregate in concrete applications (2000–2017). Construction and Building Materials, 172, 272–292.

[13] Saez del Bosque, I. F., Zhu, W., Howind, T., et al. (2017). Properties of interfacial transition zones (ITZs) in concrete containing recycled mixed aggregate. Cement and Concrete Composites, 81, 25–34.

[14] Konsta-Gdoutos, M. S., Metaxa, Z. S., & Shah, S. P. (2010). Highly dispersed carbon nanotube reinforced cement based materials. Cement and Concrete Research, 40(7), 1052–1059.

[15] Sobolkina, A., Mechtcherine, V., Khavrus, V., et al. (2012). Dispersion of carbon nanotubes and its influence on the mechanical properties of the cement matrix. Cement and Concrete Composites, 34(10), 1104–1113.

[16] Shi, X., Park, P., Rew, Y., et al. (2020). Constitutive behaviors of steel fiber reinforced concrete under uniaxial compression and tension. Construction and Building Materials, 233, 117316.

[17] Guler, S., Oker, B., & Akbulut, Z. F. (2021). Workability, strength and toughness properties of different types of fiber-reinforced wet-mix shotcrete. Structures, 31, 781–791.

[18] Wang, B., Yan, L., Fu, Q., et al. (2021). A comprehensive review on recycled aggregate and recycled aggregate concrete. Resources, Conservation and Recycling, 171, 105565.

[19] Le Hoang, A., & Fehling, E. (2017). Influence of steel fiber content and aspect ratio on the uniaxial tensile and compressive behavior of ultra high performance concrete. Construction and Building Materials, 153, 790–806.

[20] Ren, Q., Pacheco, J., de Brito, J., et al. (2024). Analysis of the influence of the attached mortar's geometry on the mechanical behaviour of recycled aggregate concrete through mesoscale modelling. Engineering Fracture Mechanics, 297, 109876.

[21] Chen, Q., Zhang, J., Wang, Z., et al. (2024). A review of the interfacial transition zones in concrete: Identification, physical characteristics, and mechanical properties. Engineering Fracture Mechanics, 300, 109979.

[22] Guo, S., Ding, Y., Zhang, X., et al. (2024). Tensile properties of steel fiber reinforced recycled concrete under bending and uniaxial tensile tests. Journal of Building Engineering, 96, 110467.

[23] Ren, Q., Pacheco, J., & de Brito, J. (2024). Mesoscale modelling of recycled aggregate concrete: A parametric analysis of properties of mesoscopic phases of RAC. Journal of Cleaner Production, 478, 143967.

[24] Zhang, J., Chen, S., Gu, F., et al. (2025). Multi-scale reinforcing effect of steel-PVA fibers and carbon nanotubes on fully recycled aggregate concrete: Mechanical properties and microstructures. Journal of Building Engineering, 113, 114067.

[25] Wang, C., Yuan, J., Lu, B., et al. (2024). New insights into the mechanical behavior and enhancement mechanism of micro-steel-fiber-reinforced recycled aggregate concrete through in-situ 4D CT analysis. Construction and Building Materials, 438, 137111.

[26] Wang, S., Qu, Y., Li, J., et al. (2025). Interfacial bonding properties between steel fiber and cement paste containing SiO_2 nanoparticles: Experimental and numerical investigation. Construction and Building Materials, 499, 144018.

[27] Cui, X., Chen, M., Feng, J., et al. (2025). Effect of cryogenic temperature on compressive and splitting tensile behaviour of industrial-recycled hybrid steel fiber reinforced ultra-high performance shotcrete. Construction and Building Materials, 479, 141445.

[28] Wang, F., & Gao, D. (2023). Tensile behavior analysis and prediction of steel fiber recycled fine aggregate concrete. Structures, 55, 2232–2248.

[29] Tang, Y., Xiao, J., Zhang, H., et al. (2022). Mechanical properties and uniaxial compressive stress-strain behavior of fully recycled aggregate concrete. Construction and Building Materials, 323, 126546.